Published OnlineFirst April 20, 2010; DOI: 10.1158/0008-5472.CAN-09-4354
Published OnlineFirst on April 20, 2010 as 10.1158/0008-5472.CAN-09-4354

Cancer Research

Tumor-Initiated Inflammation Overrides Protective Adaptive Immunity in an Induced Melanoma Model in Mice

Saïdi M. Soudja[1,2,3], Maria Wehbe[1,2,3], Amandine Mas[1,2,3], Lionel Chasson[1,2,3], Céline Powis de Tenbossche[4], Ivo Huijbers[4], Benoît Van den Eynde[4], and Anne-Marie Schmitt-Verhulst[1,2,3]

Abstract

We studied the effect of the immune system on two differentially aggressive melanomas developing in mice on conditional deletion of the *INK4A/ARF* tumor suppressor gene, with concomitant expression of oncogene *H-Ras*^{G12V} and a natural cancer-germline tumor antigen (TA). "Slow progressor" melanomas contained no activated T lymphocytes (TL). In contrast, "aggressive" melanomas were infiltrated by activated TLs lacking effector molecules and expressing high levels of PD-1, indicating an exhausted phenotype. Aggressive melanomas were also infiltrated by immature myeloid cells (IMC). Infiltration was associated with local inflammation and systemic Th2/Th17-oriented chronic inflammation that seemed to impair further activation of TLs, as tumor-specific T cells adoptively transferred into mice bearing aggressive melanomas were poorly activated and failed to infiltrate the melanoma. This immunosuppression also led to the incapacity of these mice to reject inoculated TA-positive tumors, in contrast to slow-progressing melanoma-bearing mice, which were responsive. To test the role of adaptive immunity in tumor progression, we induced melanomas in immunodeficient RagKO compound mice. These mice developed aggressive but not slow-progressing melanomas at a higher frequency and with a shorter latency than immunocompetent mice. Immunodeficient mice also developed abnormal inflammation and infiltration of IMCs in a manner similar to immunocompetent mice, indicating that this phenotype was not dependent on adaptive immunity. Therefore, tumor-intrinsic factors distinguishing the two melanoma types control the initiation of inflammation, which was independent of adaptive immunity. The latter delayed development of aggressive melanomas but was overridden by inflammation. *Cancer Res; 70(9); 3515–25. ©2010 AACR.*

Introduction

The discovery of melanoma antigens recognized by autologous T lymphocytes (TL) has led to clinical protocols designed to mobilize tumor antigen (TA)–specific TL in patients with melanoma by vaccination or by adoptive transfer of TA-specific TL. The efficacy of these treatments remains poor (1–3). Naive CD8 TL must differentiate to acquire lytic enzyme-containing granules and the capacity to secrete cytokines. TA-specific TL may undergo incomplete maturation (4) or be tolerized on encounter with the TA (5). A class of CD4 TL, called regulatory TL (Treg), is increased in many human tumors, including melanoma, and may impede tumor-specific TL maturation (6). Alternatively, tumor-intrinsic mediators may exert suppressive effects on tumor-infiltrating TL.

Another suggested mechanism of tumor escape is the accumulation of immature myeloid cells (IMC), also called myeloid-derived suppressor cells (MDSC), in cancer patients and in tumor-bearing mice (see refs. 7–9 for review). IMCs/MDSCs are a heterogeneous mixture of myeloid cells. The nature of the suppressor cell population and mechanisms of suppression may depend on the tumor and tumor-derived factors (7–9). Among myeloid cells, tumor-associated macrophages were found to either hinder or potentiate tumor progression depending on whether they express a M1 or a M2 polarization program (10).

Most models of anticancer immunotherapy use transplantable tumors. These may not recapitulate the changes in microenvironment associated with *in situ* tumor progression (11, 12). Alternative models include chemically induced neoplasms or spontaneous tumor development in aged animals (13). The TA expressed by these tumors are unknown, so specific antitumor responses are difficult to characterize. Genetically engineered cancer models were more recently designed to express viral antigens, which are also oncogenes (5, 14, 15). In these models, the TA is foreign to the host and may elicit strong adaptive immune responses, contributing to inflammation (15).

Authors' Affiliations: [1]Centre d'Immunologie de Marseille-Luminy, Université de la Méditerranée; [2]Institut National de la Sante et de la Recherche Medicale, U631; [3]Centre National de la Recherche Scientifique, UMR6102, Marseille, France and [4]Ludwig Institute for Cancer Research and Cellular Genetics Unit, Université Catholique de Louvain, Brussels, Belgium

Note: Supplementary data for this article are available at Cancer Research Online (http://cancerres.aacrjournals.org/).

Current address for I. Huijbers: The Institute of Cancer Research, London SW3 6JB, United Kingdom.

Corresponding Author: Anne-Marie Schmitt-Verhulst, Centre d'Immunologie de Marseille-Luminy, Case 906, 13288 Marseille, Cedex 9, France. Phone: 33-491269406; Fax: 33-491269430; E-mail: verhulst@ciml.univ-mrs.fr.

doi: 10.1158/0008-5472.CAN-09-4354

Published OnlineFirst April 20, 2010; DOI: 10.1158/0008-5472.CAN-09-4354

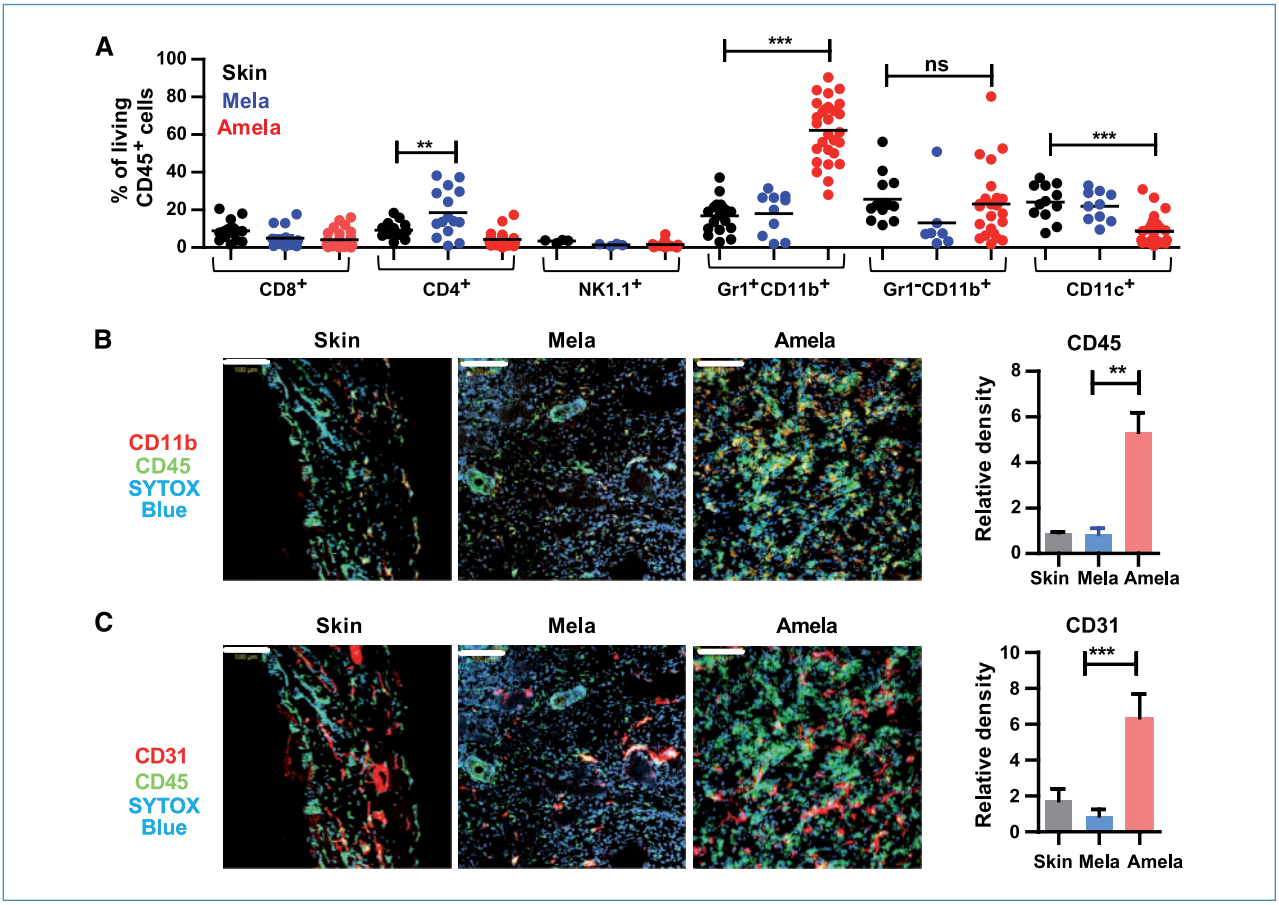

Figure 1. CD11b$^+$Gr1$^+$ cell-enriched leukocytes infiltrate induced aggressive Amela but not slow progressor Mela tumors. A, Mela or Amela tumors from OHT-induced TiRP-*10B;Ink4a/Arf*$^{flox/flox}$ (TiRP) mice or skin from OHT-treated *Ink4a/Arf*$^{flox/flox}$ littermate TiRP-negative (control) mice were treated for FACS analysis. B and C, a portion was snap frozen for immunohistology. Data in A represent the % of each leukocyte population within the CD45$^+$ live cell fraction. In B and C, immunohistology shows SYTOX Blue staining for nuclei (blue) and anti-CD45.2 staining for leukocytes (green) together with anti-CD11b staining (red in B) or anti-CD31 staining (red in C). In B, CD11b$^+$CD45$^+$ cells appear yellow. Scale bars, 100 μm. The relative density (fraction area) of CD45$^+$ (B) and CD31$^+$ (C) cells detected in skin, Mela, and Amela tumors was evaluated from immunohistologic slides using NIH ImageJ software. Columns, mean of at least three sections in four separate experiments; bars, SD. A Student's *t* test between groups was performed to assess statistical significance. ***, $P < 0.001$; **, $P < 0.01$; *, $P < 0.1$; $P > 0.1$, nonsignificant (ns).

We described a mouse model of sporadic melanoma based on conditional deletion of tumor suppressor genes with concomitant expression of a natural mouse TA. This model allows tracking of TA expression in the host using CD8 TL expressing a TA-specific T-cell receptor (TCR). The chosen TA, encoded by an X-linked "cancer-germline" gene named *P1A*, shares with human cancer-germline counterparts an expression pattern restricted to germinal cells (3, 16). This category of TA was recently also detected in the thymus (17) and leads to a partially deleted T-cell repertoire characteristic of cancer-germline TA.[5]

We reported two types of cutaneous tumors expressing P1A developing in induced mice: pigmented melanomas that grow slowly and less pigmented, more aggressive tumors (18). We here characterized the status of the immune system in mice bearing either of the melanomas and addressed the contribution of adaptive immunity in the inflammation associated with the aggressive melanoma. We show that tumor-intrinsic factors differentiate these melanoma types and control the initiation of inflammation, which was independent of adaptive immunity.

Materials and Methods

Mice. TiRP-*10B;Ink4a/Arf*$^{flox/flox}$ mice, "TiRP mice," previously described on a mixed genetic background (18), were backcrossed to B10.D2 (B10.D2/nOlaHsd, H-2^d; Harlan) for >10 generations (see Supplementary Materials and Methods for details). TiRP mice devoid of adaptive immunity by crossing with Rag-1*KO* B10.D2 (RagKO) mice are called TiRP RagKO mice. Mice heterozygous for the H-2L^d/P1A$_{35-43}$–specific TCR transgene were kept on the RagKO background (TCRP1A RagKO; ref. 19). Treatment of TiRP mice with 4OH-tamoxifen

[5] I. Huijbers, S.M. Soudja et al. in preparation.

Published OnlineFirst April 20, 2010; DOI: 10.1158/0008-5472.CAN-09-4354

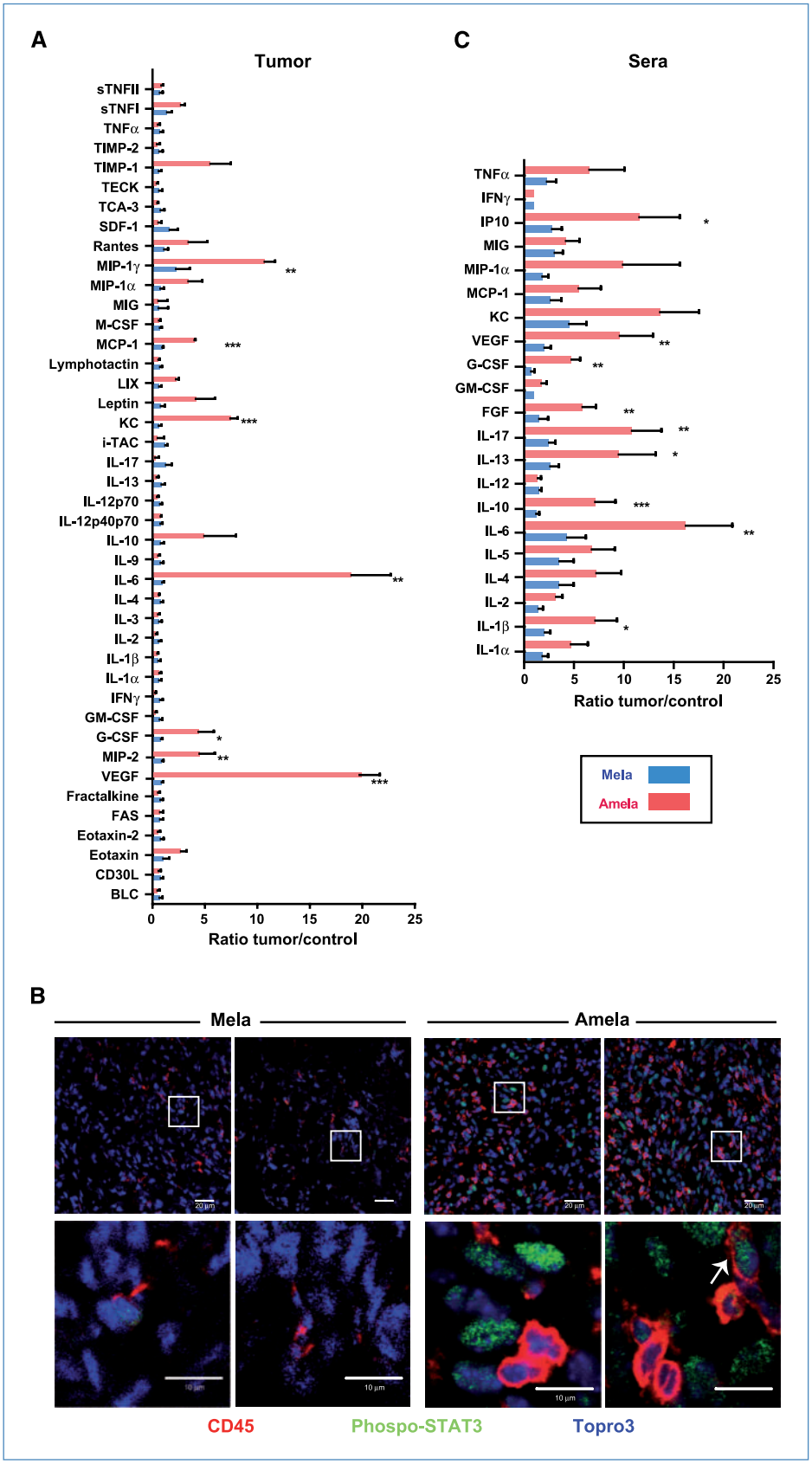

Figure 2. Inflammatory cytokines detected in the tumor microenvironment and systemically in mice with induced aggressive Amela tumors. A, dissociated Mela or Amela tumors from OHT-induced TiRP mice or skin from OHT-treated littermate TiRP-negative control mice were cultured for 48 h and the content of the supernatants of cytokines was measured by "inflammatory cytokine array," except VEGFA and MIP-2, which were assayed by ELISA. Results are expressed as ratio of the values obtained in tumor versus skin supernatants (from at least three different samples). B, immunohistology of Mela (left) and Amela (right) tumors shows Topro staining for nuclei (blue) and anti-CD45.2 staining for leukocytes (red) together with anti-phospho-tyrosine-STAT3 staining (green). White arrow, $CD45^+$ phospho-tyrosine-STAT3–positive cell. Scale bars, 20 μm (top) and 10 μm (bottom). In the presence of phospho-tyrosine-STAT3 peptide, no staining was observed (Supplementary Fig. S1E). Results are representative of three distinct tumors of each type. C, sera collected from OHT-treated littermate control mice (8 mice) or induced Mela- or Amela-bearing mice (11 mice of each group) were tested for cytokine content using Luminex technology (except G-CSF, which was assayed by ELISA) and results are expressed as ratio of the values for tumor-bearing versus control mice sera. *P* values are as before.

Published OnlineFirst April 20, 2010; DOI: 10.1158/0008-5472.CAN-09-4354

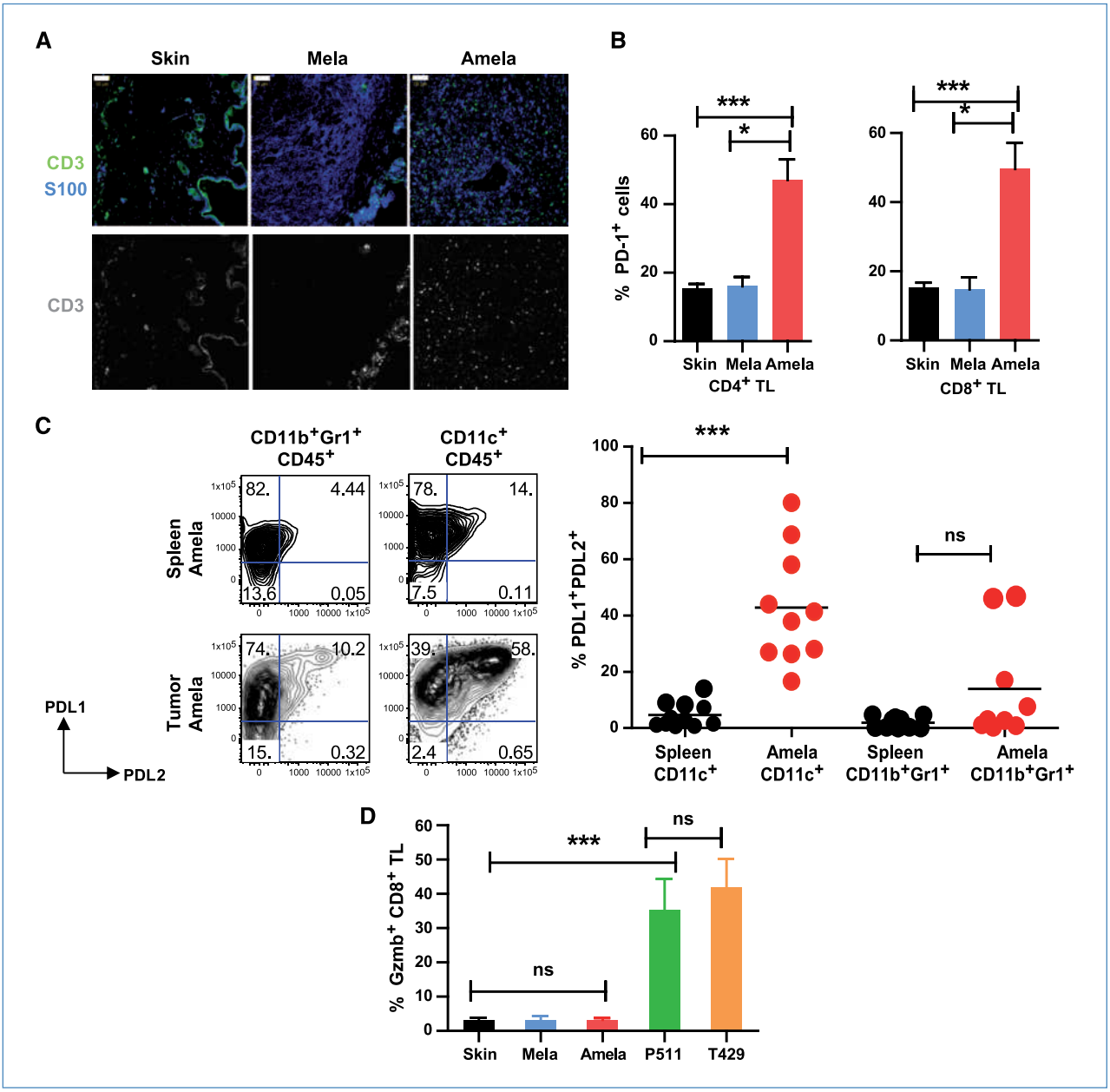

Figure 3. Location and phenotype of endogenous TL infiltrates in induced Amela melanomas. TLs in induced Mela or Amela tumors were compared with those present in skin of littermate control (n = 4) mice by immunohistology (A) and by FACS analysis (B and D). A, anti-S100 staining (blue) of melanomas (18) and anti-CD3ε staining (green) of TL show that TLs are outside the tumor in Mela but infiltrate the Amela melanomas (bottom shows anti-CD3ε staining in white). Scale bars, 50 μm. B, data show % PD-1$^+$ cells among CD4 (left) or CD8 (right) TLs from skin or tumor analyzed as in Fig. 1A. C, expression of PD-1 ligands PDL1 and PDL2 on splenic (top graphs) or tumor-infiltrating (bottom graphs) CD11b$^+$Gr1$^+$ (left) and CD11c$^+$ (right) populations present in induced Amela-bearing mice. Dot graph shows % PDL1$^+$PDL2$^+$ cells within each of the indicated populations for 10 individual mice. D, data show % Gzmb$^+$ cells among CD8 TL from skin or tumor analyzed as in B with additional samples from transplanted P1A-positive mastocytoma P511 and melanoma T429 (see Materials and Methods) 7 d after tumor inoculation, respectively, in F1 or in B10.D2 mice (see Materials and Methods). Data are representative of four (A), five (B), and eight (D) mice in each group.

(OHT; Sigma) was as described (18). DBA/2 mice (Charles River) were crossed with B10.D2 mice and F1 litters were used in some tumor transplantation experiments, as indicated. All procedures were preapproved by the Regional Committee on Ethics for Animal Experimentation, in accordance with French and European directives. Mice were housed under specific pathogen-free conditions.

Immunohistology. Skin or tumors were snap-frozen in Tissue-Tek (Sakura Finetek). Frozen sections were fixed in acetone and stained with the indicated antibodies. Before

Published OnlineFirst April 20, 2010; DOI: 10.1158/0008-5472.CAN-09-4354

staining with anti-phospho-tyrosine-signal transducer and activator of transcription 3 (STAT3) antibodies, cells were additionally permeabilized with methanol. Confocal microscopy and image processing were performed, respectively, with a Zeiss LSM150 microscope and Zeiss LSM software. Immunofluorescence was quantified using NIH ImageJ software for the determination of relative densities of a given marker within a fixed section (fraction area).

Antibodies and MHC tetramers. For immunohistology, anti-CD45.2-FITC (104; Fig. 1), anti-CD11b-APC (M1/70), anti-CD31-PE (390), anti-CD3ε-FITC (2C11), and anti-CD45.2-biotinylated/streptavidin-Alexa546 (Fig. 2) from BD Biosciences; anti-phospho-tyrosine-STAT3 (Cell Signaling Technology); anti-(rabbit Ig)-Alexa488; anti-S100 (Dako); and anti-(rabbit Ig)-Alexa647 (Molecular Probes) were used.

For flow cytometry, monoclonal antibody (mAb) anti-Gr1-PE-Cy7 (RB6-8C5), anti-CD11b-PerCP-Cy5.5, anti-CD11c-APC (HL3), anti-CD4-FITC (RM4-5), anti-CD8α-PerCP (Fig. 5A and B) or anti-CD8α-Pacific Blue (Figs. 1–3; 53-6.7), anti-NK1.1-APC (PK136), anti-CD44-APC (IM7), and anti-PD-1-PE (J43) were from BD Biosciences and anti-CD45.2-Alexa700, anti-Ter119-FITC, anti-PDL1-biotinylated (MIH5) plus streptavidin-FITC, and anti-PDL2-PE (TY25) were from eBioscience. PE-labeled H-2L^d/P1A tetramers (20) were a kind gift of Didier Colau (Université Catholique de Louvain, Brussels, Belgium).

Flow cytometry. For tumors or normal skin, tissues were dissected and digested with 0.05 mg/mL collagenase IV (Roche) plus 1 mg/mL collagenase I (Roche) and 0.01 mg/mL DNase I (Roche) in RPMI 1640/10% FCS for 30 minutes at 37°C. Samples were then minced and filtered through a 70-μm nylon mesh. RBCs were lysed with NH_4Cl. Fc receptors were blocked by anti-CD16/CD32 mAb 2.4G2. Samples were labeled with mAb (as indicated) plus "Live/Dead Fixable Aqua Dead Cell" dye ("vivid" from Invitrogen). Gating was on the CD45.2-positive and vivid-negative population, in which further markers were analyzed. Analyses of cell populations from lymphoid organs were as described (20). For granzyme B (Gzmb) intracellular staining, TLs were labeled with surface-binding mAbs, then permeabilized with Fix/Perm buffer (eBioscience), and labeled with anti-Gzmb mAb (Invitrogen). For IFNγ intracellular staining, TLs were preactivated with phorbol 12-myristate 13-acetate (PMA; 10 ng/mL; Sigma-Aldrich) and ionomycin (200 ng/mL; Sigma-Aldrich) in the presence of monensin (GolgiStop; BD Pharmingen) for 4 hours or with P1A$_{35–43}$ peptide (1 μmol/L; LPYLGWLVF) overnight at 37°C in RPMI 1640/10% FCS. Washed cells were treated for intracellular staining (anti-IFNγ-APC; BD Biosciences) after labeling with surface-binding mAb. Flow cytometry was performed on either LSRI, CANTO II, or LSR II (BD Biosciences), and data were analyzed using FlowJo software (Tree Star).

Adoptive transfer experiments. Naive TCRP1A TLs isolated from lymph node (LN) and spleen of TCRP1A RagKO mice were labeled with the intracytoplasmic dye 5,6-carboxyfluorescein diacetate succinimidyl ester (CFSE; Molecular Probes), and 3×10^6 cells in 100 μL PBS were injected retroorbitally in mice. Six days later, mice were sacrificed for analysis of TL divisions after gating on H-2L^d/P1A tetramer-binding CD8 TL, as described (20).

Cytokine detection. Supernatant fluids obtained after incubating freshly isolated tumor or normal skin cells (2.5×10^5/mL) at 37°C for 48 hours were stored at −80°C. Assays used for cytokine detection in supernatants or in sera are described in Supplementary Materials and Methods.

Melanoma cell lines. Established in culture from melanomas developing in TiRP mice as described (18), melanoma cell lines were further cultured in RPMI 1640 complete medium. The expression of *H-Ras^{G12V}* and *P1A* transcripts by these cells (Supplementary Fig. S6A–C) as well as the deletion of the *Ink4a/Arf* gene (genomic PCR; Supplementary Fig. S6D; ref. 18) were verified for each line. Line T429 was used in transplantation experiments.

Tumor transplantation and monitoring. P1A-expressing T429 Amela tumor line and mastocytoma P815 (H-2^d, of DBA/2 origin) subline P511 were transplanted s.c. (10^6 cells), respectively, in mice on the B10.D2 genetic background (or TiRP or TCRP1A RagKO mice, as indicated) or in F1(B10.D2×DBA/2) mice, and their growth was monitored with a caliper, as described (20).

Statistical analyses. Statistical analyses were performed with the Student's *t* test using GraphPad, and two-tailed *P* values are given as follows: *, $P < 0.1$; **, $P < 0.01$; and ***, $P < 0.001$.

Results

Two types of melanomas develop following deletion of Ink4a and expression of H-Ras^{G12V} in melanocytes. Genetic lesions in melanoma frequently include disruption of INK4A/ARF tumor suppressors and activation of the mitogen-activated protein kinase pathway (21). Mice lacking expression of the *Ink4a/Arf* locus that simultaneously express activated H-Ras^{G12V} under control of a melanocyte-specific promoter develop melanomas at high frequency but also fibrosarcomas due to ubiquitous loss of Ink4a/Arf expression (22).

Here, we studied melanoma development in the previously described TiRP mice (Supplementary Materials and Methods; ref. 18). In this model, the conditional "Cre-estrogen receptor/LoxP" technology was applied to restrict the *Ink4a/Arf* deletion and the expression of both *H-Ras^{G12V}* and the natural TA *P1A* to melanocytes (18). Melanomas are induced in ∼40% of the mice by treatment with OHT. Some are heavily melanotic melanomas (designated "Mela"), growing slowly (∼10 mm^3/d), resulting in death within 3 months. Most induced melanomas are nonpigmented (designated "Amela") and more aggressive (growing ∼100 mm^3/d), resulting in death of mice within 1 month. A minority of mice develop a melanotic tumor with subsequent amelanotic growth at the same site ("double melanomas"). Differences in the incidence of pigmented versus nonpigmented tumors in the present versus our previous (18) report are probably related to genetic background and/or environmental differences (Supplementary Materials and Methods). All tumors expressed H-Ras^{G12V} and the TA P1A (18), detectable by CD8 TL from TCRP1A transgenic mice specific for the P815A P1A epitope in association with the H-2L^d molecule (18, 19).

Published OnlineFirst April 20, 2010; DOI: 10.1158/0008-5472.CAN-09-4354

Amela tumor progression is associated with leukocyte infiltration. A comparison of hematopoietic cells ($CD45^+$) present in the stroma of the two types of induced melanoma and in normal skin of littermate mice showed that lymphocyte populations (NK, CD4, and CD8 TL) were not enriched in the melanomas, except for a slight increase in CD4 TL in Mela tumors (Fig. 1A). A significant increase in $CD11b^+$ cells (characterizing the myeloid lineage) was observed in Amela tumors, however. The population of $CD11b^+Gr1^+$ cells, a phenotype akin to IMC/MDSC, represented ~70% of the $CD45^+$ population in the Amela tumors compared with ~20% in Mela tumors and in normal skin (Fig. 1A). In contrast, the $CD11c^+$ population, corresponding to dendritic cell (DC), was relatively decreased in Amela tumors (Fig. 1A). Immunohistology confirmed much denser infiltration of $CD45^+$ and CD11b cells in Amela compared with Mela tumors (Fig. 1B).

Leukocyte infiltration correlated with a high vessel density in aggressive Amela compared with Mela melanomas or healthy skin (anti-CD31 antibody; Fig. 1C). We analyzed whether inflammatory cytokines are secreted in the tumor microenvironment.

Amela tumor progression is associated with inflammation, splenomegaly, and myeloproliferative disorders. Supernatant fluids from freshly explanted tumor cells or from control mice skin cells were collected after 48 hours. Some inflammatory cytokines [interleukin (IL)-6 and IL-10] as well as chemokines (MCP-1/CCL2, KC/CXCL1, Mip-1γ/CCL9, and Mip-2/CXCL2) and growth factors [granulocyte colony-stimulating factor (G-CSF) and vascular endothelial growth factor A (VEGFA)] were found almost exclusively in supernatants of the Amela tumors (Fig. 2A; Supplementary Fig. S1A and B).

Consistent with the detection of cytokines capable of activating STAT3 (IL-6, IL-10, and VEGFA) and of being upregulated on STAT3 activation (IL-6, IL-10, VEGFA, and MCP-1/CCL2; ref. 23), we observed nuclear phospho-STAT3 in Amela tumor cells and in some infiltrating CD45 leukocytes but not in Mela tumors or in their infiltrates (Fig. 2B; Supplementary Fig. S1E). By Luminex analysis (Fig. 2C; Supplementary Fig. S1D), increased expression in sera from Amela-bearing mice was found for growth factors [G-CSF, VEGFA, and fibroblast growth factor b (FGFb)/FGF2] capable of mobilizing myeloid precursor cells from the bone marrow (BM; refs. 24, 25), for chemokines capable of recruiting such cells (KC/CXCL1 and IP-10/CXCL10), and for immunomodulating cytokines (IL-6, IL-10, IL-13, and IL-17). Cytokines known to promote Th1/CTL responses, such as IL-12 and IFNγ, were not detected in supernatant fluids from tumors *ex vivo* (Supplementary Fig. S1A) and were not increased in sera of Amela-bearing mice (Fig. 2C; Supplementary Fig. S1D). Rather, these sera contained components capable of promoting Th17/Tc17-type (IL-6 and IL-17; refs. 26, 27) or Th2/Tc2-type (IL-10 and IL-13; ref. 28) responses.

As described in inflammation (29, 30), systemic alterations in hematopoiesis were present in mice with induced melanomas. Amela-bearing, but not Mela-bearing, mice suffer from splenomegaly (Supplementary Fig. S2A) with accumulation of IMC ($CD11b^+Gr1^+$) in spleen and LN (Supplementary Fig. S2C, D, and F). In blood, $CD11b^+Gr1^+$ cell numbers were also increased, whereas lymphocyte counts were unchanged (Supplementary Fig. S2G). BM cells were relatively depleted of $Ter119^+$ erythroid precursors (Supplementary Fig. S3), associated with extramedullary (splenic) hematopoiesis (increased proportion of $CD45^-Ter119^+$ cells; Supplementary Fig. S2B and E). Splenic lymphocytes were underrepresented as a % of $CD45^+$ cells relative to $CD11b^+$ myeloid cells, but their total numbers were marginally increased (Supplementary Fig. S2B).

Location and phenotype of endogenous TL infiltrating induced Amela melanomas. Expression of genes associated with a Th1/CTL phenotype such as Gzmb, when associated with tumor infiltration by TL, was prognostically favorable in colorectal cancer patients (31). Tumor-infiltrating myeloid-derived cells, on the other hand, have been associated with potentially TL-suppressive activities (7, 8). Among these, arginine depletion (7) might be involved in the Amela tumor microenvironment because arginase-1 and cox2/ptgs2 (32) could be detected in the Amela tumors (Supplementary Fig. S4A and B).

Immunohistology of tumors of induced melanoma-bearing mice (Fig. 3A) clearly showed that endogenous TL had infiltrated Amela, whereas they remained at the edge of Mela tumors. Fluorescence-activated cell sorting (FACS) analysis revealed that a majority of the skin or tumor-infiltrating CD4 and CD8 TL had an antigen-experienced phenotype, $CD44^{high}$ $CD62L^-$, in comparison with the TL located in tumor-draining LN (Supplementary Fig. S5A).

In contrast, PD-1, a molecule present on impaired immune TL in chronic disease (33), was expressed on tumor-infiltrating CD4 and CD8 TL in Amela, but not in Mela, tumors nor in TL present in normal skin (Fig. 3B; Supplementary Fig. S5B). Furthermore, about half of the $CD11c^+$ DC infiltrating the Amela tumors expressed both PD-1 ligands PDL1 and PDL2, whereas $PDL1^+PDL2^+$ cells constitute a minor population of splenic DC (Fig. 3C), indicating that antigen-presenting cells in the tumor microenvironment may favor engagement of the TL-expressed PD-1. Among $CD11b^+Gr1^+$ cells, few were $PDL1^+PDL2^+$, however (Fig. 3C).

None of the CD8 TL present in Amela infiltrates expressed Gzmb, whereas ~35% of those infiltrating transplanted P1A-expressing mastocytoma P511 or T429 melanoma lines (see Materials and Methods) did (Fig. 3D). Furthermore, in contrast to CD8 TL isolated from the P511 tumor, Amela-infiltrating CD8 TL failed to produce IL-2 on *in vitro* stimulation with PMA and ionomycin (Supplementary Fig. S5D), suggesting that these TLs might be anergized. Melanoma-infiltrating TLs in patients are also functionally impaired, although some express Gzmb (34, 35).

In the CD4 TL compartment, a significant increase in $Foxp3^+$ TL was observed in the LN draining Amela compared with Mela tumors as well as in the Amela tumor compared with skin or control LN of aged-matched control mice (Supplementary Fig. S5E–G). This population may also contribute to the inactivation of CD8 TL (6).

Altogether, the data suggest that the Amela tumors have been infiltrated by TLs that have been chronically stimulated, leading to their "exhaustion." In contrast, the Mela tumors were surrounded by TL, which did not acquire an "exhausted" phenotype (Fig. 3A and B).

Published OnlineFirst April 20, 2010; DOI: 10.1158/0008-5472.CAN-09-4354

Table 1. Incidence and latency of melanoma development after OHT treatment of TiRP and TiRP RagKO mice (see Materials and Methods)

Mice	TiRP				TiRP RagKO			
Melanomas	Mela (pigmented)	Amela (unpigmented)	Mela/ Amela (double)	Total	Mela (pigmented)	Amela (unpigmented)	Mela/ Amela (double)	Total
Incidence, number (%)	29 (8.0%)	94 (26.0%)	21 (5.8%)	144/361 (40.0%)	0 (0%)	9 (75.0%)	0 (0%)	9/12 (75.0%)
Latency (d)	159 ± 22	163 ± 17				68 ± 4		
Growth (mm^3/d)	12 ± 8	98 ± 19				>150		

Adaptive immunity delays Amela tumor development. We asked whether an adaptive immune response might be at the origin of the inflammation in Amela-bearing mice, leading secondarily to IMC/MDSC infiltration. This was tested by analyzing TiRP mice on the RagKO background (see Materials and Methods).

The incidence of OHT-treated mice developing Amela tumors was increased in TiRP RagKO mice, and their latency was reduced (Table 1). However, no Mela or double Mela/Amela tumors were observed in these immunodeficient mice (Table 1). Mela tumor development may be masked by the rapid development of the Amela tumors in these mice (Table 1).

Because the Amela tumors developing in TiRP RagKO mice were infiltrated by $CD45^+$ leukocytes (Fig. 4A) to the same extent as in TiRP mice (legend to Fig. 4A) and these leukocytes were also enriched in $CD11b^+Gr1^+$ cells (Fig. 4A), adaptive immunity is not responsible for the recruitment of myeloid cells within the tumor, nor for the initiation of myeloproliferative disorder (MPD), because $CD11b^+Gr1^+$ cells also accumulated in the enlarged spleens of the Amela-bearing TiRP RagKO mice, which also presented extramedullary hematopoiesis, as indicated by the increased proportion of $Ter119^+$ cells (Fig. 4B).

Altogether, these data indicate that adaptive immunity lowers the incidence and delays the development of induced aggressive Amela, but not of Mela, tumors, suggesting a protective role for adaptive immunity against development of the former. They also establish that adaptive immunity is not responsible for the initiation of inflammation in the Amela-bearing mice.

Failure of adoptively transferred P1A-specific CD8 TL to infiltrate the induced Amela tumor. To address whether

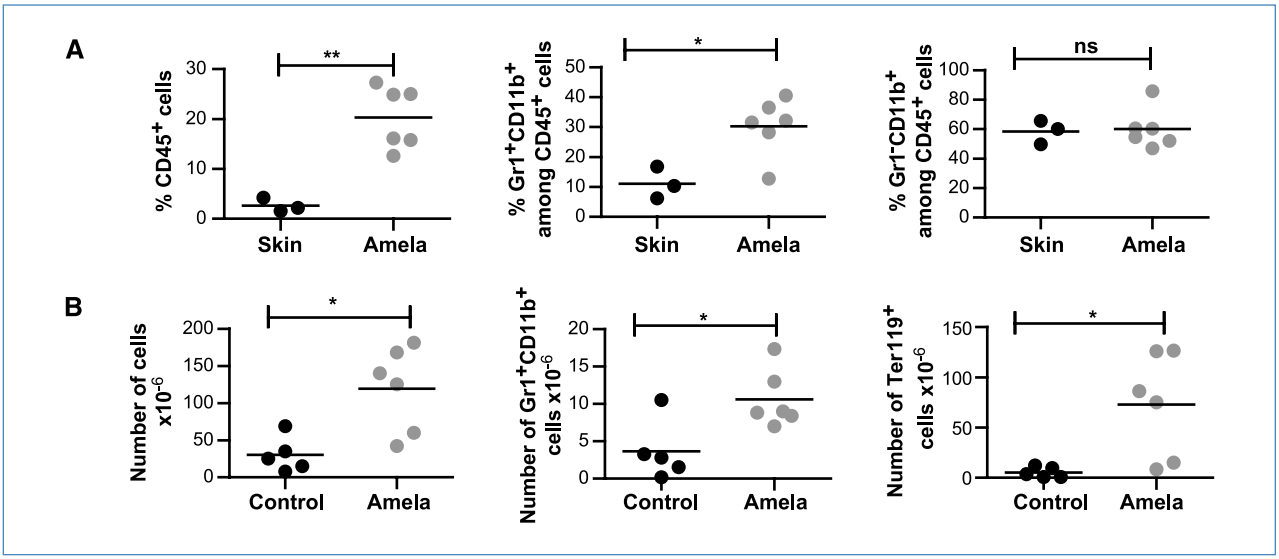

Figure 4. Adaptive immunity delays the development of aggressive melanomas, but inflammation was established independently of adaptive immune reactivity. A, leukocyte infiltration in Amela tumors developed in TiRP RagKO mice. Skins of RagKO control mice (Skin) or Amela tumors induced in TiRP RagKO mice (Amela) were analyzed by FACS for expression of CD45, CD11b, and Gr1 after gating on live cells. Data show % $CD45^+$ cells among live cells (left), % $CD11b^+Gr1^+$ cells (middle), and % $CD11b^+Gr1^-$ cells (right) among $CD45^+$ cells. For comparison, in immunocompetent TiRP mice, % $CD45^+$ cells among live cells were 16.3 ± 2.5 (n = 11) in induced Amela tumors and 4.4 ± 1.0 (n = 7) in control mice skin. B, splenic populations from TiRP RagKO mice with induced Amela tumors (Amela) or littermate control mice (Control). Increased splenic cellularity (left) and number of $CD11b^+Gr1^+$ (middle) or $CD45^-Ter119^+$ (erythroid precursors; right) cells are shown. P values are as before.

Published OnlineFirst April 20, 2010; DOI: 10.1158/0008-5472.CAN-09-4354

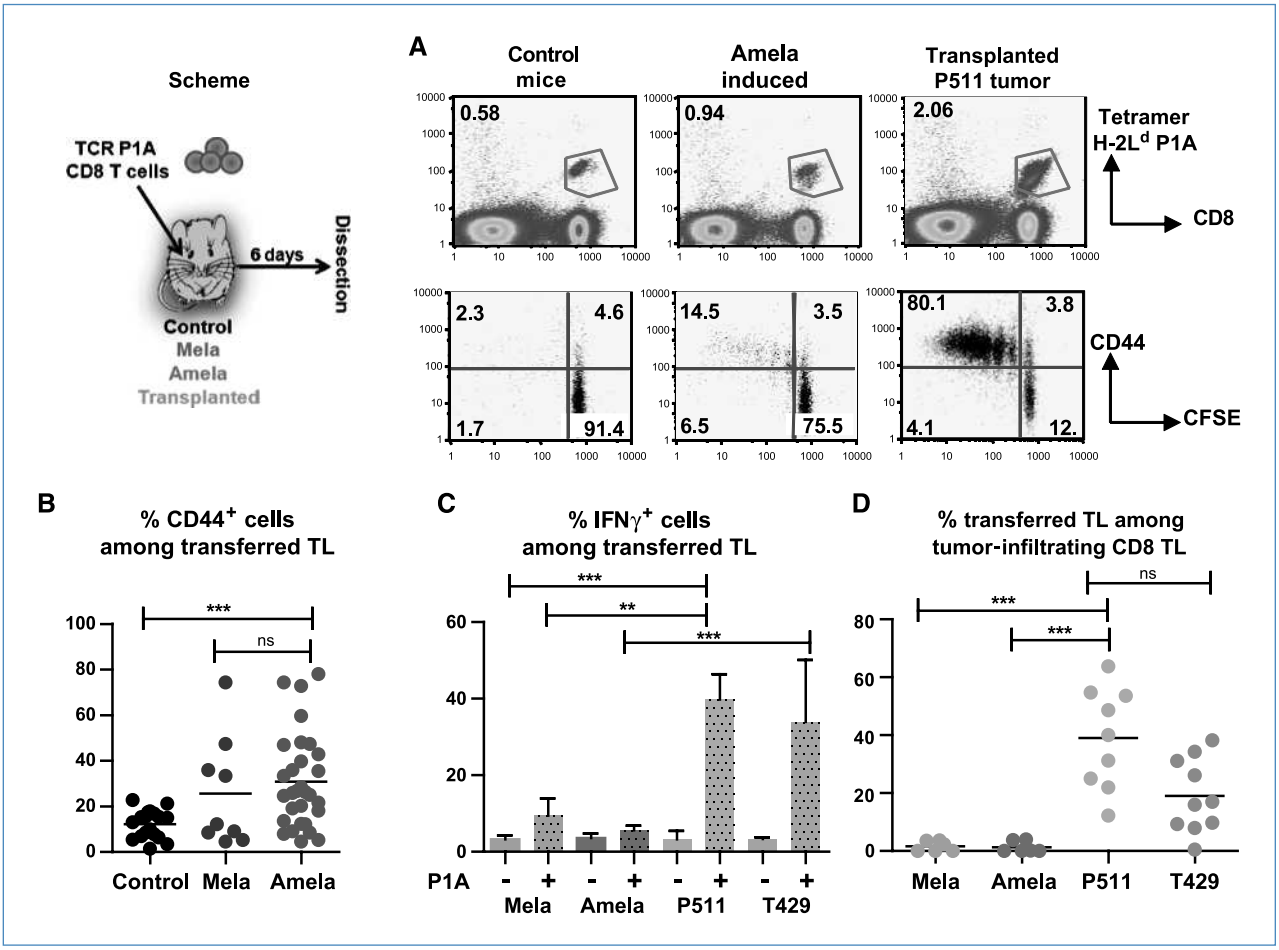

Figure 5. Impaired activation of adoptively transferred P1A-specific CD8 TL in both induced Mela- and Amela-bearing mice. A to D, CFSE-labeled (3×10^6) TCRP1A CD8 TLs were transferred i.v. in induced melanoma-bearing TiRP mice (Mela and Amela) and in control tumor-free mice (Control), as well as in mice transplanted (10^6 cells s.c.) with P1A-positive mastocytoma P511 (A, C, and D) or melanoma line T429 (C and D) 5 d earlier. Cells from tumor-draining LN were analyzed by cytofluorimetry 6 d after TL transfer. A, FACS staining for H-2L^d/P1A tetramer versus CD8 (top graphs) and CD44 versus CFSE on tetramer$^+$ CD8 TL (bottom graphs). B, % CD44$^+$ TL among tetramer$^+$CD8$^+$ TL for a number of experiments. C, labeling with H-2L^d/P1A tetramer and anti-CD8, followed by intracellular staining with anti-IFNγ, was performed on retrieved TL cultured *in vitro* for 10 h with (+) or without (–) P1A peptide (10^{-6} mol/L). Data expressed as % IFNγ producing tetramer$^+$ CD8 TL for five independent experiments (three for T429). D, data expressed as % tetramer$^+$ cells among tumor-infiltrating CD8 TL for independent experiments in transplanted (P511 or T429) and in induced Mela or Amela tumors. *P* values are as before.

adoptively transferred anti-TA CD8 TL might become activated in the inflammatory context existing in Amela-bearing mice, we infused naive CFSE-labeled CD8 TCRP1A TL in mice with induced or transplanted tumors and analyzed the TCRP1A TL retrieved from the tumor-draining LN 6 days later (Fig. 5). When transferred in tumor-free control mice, most of the retrieved TCRP1A TLs had retained low CD44 expression and undiluted amounts of CFSE (Fig. 5A). Among TCRP1A TL retrieved from induced melanoma-draining LN, a fraction presented an upregulation of surface CD44 and a CFSE-diluted phenotype (Fig. 5A) whether the mice carried Mela or Amela tumors (Fig. 5B). When infused in mice with transplanted P1A-expressing tumors, most TCRP1A TLs divided and acquired CD44 expression (Fig. 5A). TCRP1A TL from LN draining induced melanomas also showed poor capacity to make IFNγ (Fig. 5C and below). Importantly, in spite of a total downregulation of the LN-homing receptor CD62L from the surface of a majority of the responding TCRP1A TL (data not shown), no TCRP1A TL seemed to infiltrate the induced melanoma (Fig. 5D). This contrasts with the high degree of infiltration of TCRP1A TL in the P1A-expressing transplanted tumors (Fig. 5D). Thus, although Amela tumors had initially been infiltrated by TL, adoptively transferred CD8 TL failed to infiltrate established induced tumors.

The weaker response of TCRP1A TL to the induced Amela compared with the transplanted P511 is probably not due to a lower expression of the P1A TA because levels of *P1A* mRNA evaluated by quantitative reverse transcription-PCR were generally higher in the Amela tumors (Supplementary Fig. S6A–C). In addition, when infused in mice bearing a transplanted Amela tumor (T429, see later section), TCRP1A TL migrated efficiently to the tumor tissue (Fig. 5D) and could

Published OnlineFirst April 20, 2010; DOI: 10.1158/0008-5472.CAN-09-4354

produce IFNγ (Fig. 5C). Therefore, a suppressive environment may have developed in the induced Amela-bearing mice. To test this hypothesis, we next analyzed how induced Mela- or Amela-bearing mice reacted to transplanted P1A-positive tumors.

Mice with induced Amela tumors fail to reject a P1A-expressing melanoma. The melanoma tumor line T429, established in culture from an induced Amela tumor, was rejected on the basis of expression of P1A, as shown by its growth in RagKO mice and rejection in TCRP1A RagKO mice (Fig. 6A). Growth of this P1A-expressing transplanted melanoma was also restrained in induced Mela-bearing and littermate control mice but not in induced Amela-bearing mice (Fig. 6A). Further, CD8 TL infiltrating the transplanted T429 melanoma in induced Amela-bearing mice expressed very low levels of Gzmb, suggesting that in spite of their capacity to infiltrate the transplanted tumor these TLs did not efficiently differentiate in induced Amela-bearing mice (Fig. 6B). These results indicate that Amela tumors are immunogenic. Therefore, it is possible that an initial immune response to the Amela tumor occurred but that mice with growing induced Amela tumors were immunosuppressed, in contrast to Mela-bearing mice, which were responsive.

Discussion

Inflammation as a result of an oncogenic process or of adaptive immunity? Innate and adaptive immunity have both been implicated in resistance to spontaneous and carcinogen-induced tumors in mice (13). Alternatively, immunity/inflammation may contribute to tumor progression (10, 36). One view is that inflammation results from antitumor immune reactivity (15, 36, 37). The other is that tumor-intrinsic changes associated with the oncogenic process also involve a "proinflammatory" program (10, 38).

In human papillomavirus 16–induced tumors, antibody production seemed responsible for an inflammatory reaction with tumor-promoting effects (15). In polyoma virus middle T–induced breast cancer, macrophages recruited to the tumor were found to be essential for the angiogenic switch (39), and M2-type polarization (10, 36) of tumor-associated macrophages and IMC was recently suggested to be dependent on CD4 T cells (40).

In contrast to these deleterious tumor-promoting effects of components of adaptive immunity, in the inducible melanoma model with expression of a natural mouse TA, adaptive immunity seemed to be initially protective against Amela tumor development. The incidence of Amela tumors was considerably increased and the latency of their appearance was shortened in TiRP RagKO compared with immunocompetent TiRP mice. As MPD and IMC recruitment was also present in TiRP RagKO mice with induced Amela tumors, adaptive immunity is not responsible for the inflammation associated with the recruitment of IMC in lymphoid organs and tumor, either through classic B cells, CD4 or CD8 TL, or CD4 Treg, as suggested in spontaneous tumor models expressing foreign antigens (15, 41).

When inflammation associated with Amela tumor progression occurs, the adaptive immune system would initially become activated to TAs, explaining the higher incidence of Amela tumor development in the immunodeficient RagKO

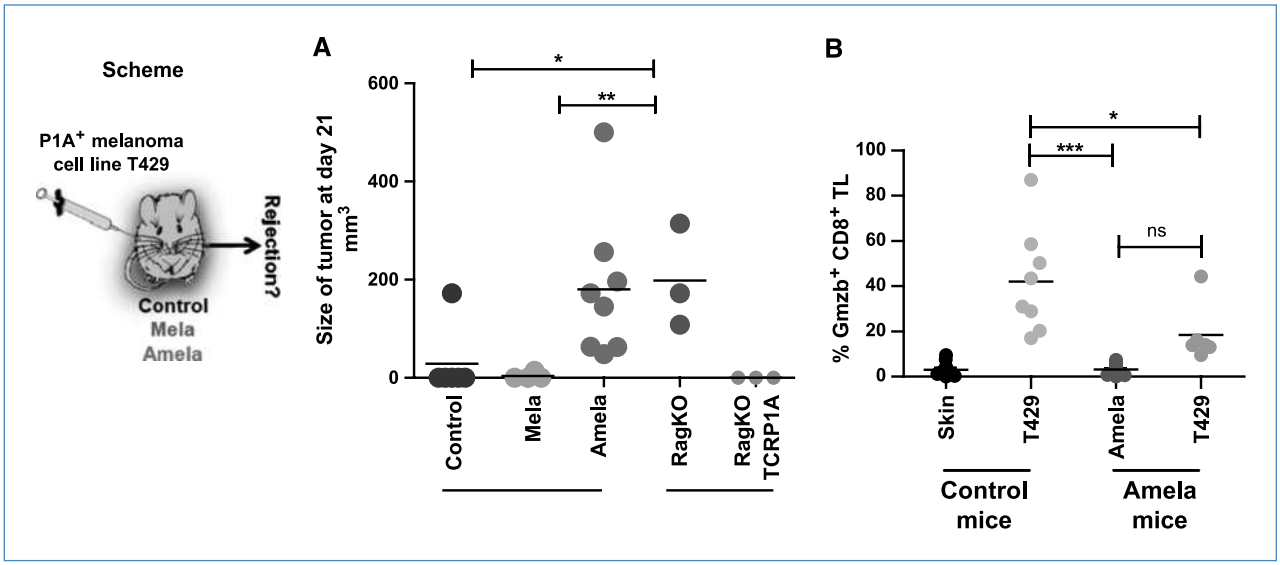

Figure 6. Failure to reject a P1A-expressing melanoma is restricted to induced Amela-bearing mice. A, TiRP mice developing either Mela or Amela induced tumors and littermate control (control) mice were injected s.c. with 1×10^6 T429 line tumor cells. T429 tumor size (as mm^3) was monitored after inoculation (see Materials and Methods). As a positive control for growth, T429 was injected in RagKO mice. P1A-dependent rejection of tumor T429 is observed in TCRP1A RagKO mice, which express a monoclonal population of P1A-specific CD8 TL. Data, expressed as size of tumor at day 21 after inoculation, were pooled from two experiments. B, induced Amela-bearing and littermate control mice injected with tumor line T429 were sacrificed, and CD8 TLs present in the skin and the transplanted T429 tumor from control mice and in induced Amela tumor and transplanted T429 tumor from the Amela-bearing mice were analyzed for expression of Gzmb by FACS. Data are expressed as % $Gzmb^+$ cells among CD8 TL. *P* values are as before.

Published OnlineFirst April 20, 2010; DOI: 10.1158/0008-5472.CAN-09-4354

TiRP mice. Subsequently, however, the extent of Amela tumor-induced inflammation amplified by myeloid cells recruited to the tumor would be such that it may "override" the initially protective adaptive immunity. Because Amela tumor cells and some Amela-infiltrating leukocytes expressed nuclear phospho-STAT3, the inflammation amplification possibly involves a STAT3-dependent feed-forward loop, as recently reported (23). This is consistent with the detection of STAT3-activating (IL-6, IL-10, and VEGFA) as well as STAT3-dependent (IL-6, IL-10, VEGFA, and MCP-1/CCL2) inflammatory mediators in the Amela tumors, as well as systemically (IL-6, IL-10, IL-17, FGF, and VEGFA).

The mechanisms by which adaptive immunity accounts for the relative resistance to Amela tumor development in immunocompetent mice remain to be established. Indeed, CD4 and CD8 TLs may initially be stimulated by TA and mount an effector response against the tumor or its stroma (42). This would be consistent with the antigen-experienced phenotype of Amela tumor-infiltrating TL, their expression of the marker PD-1 (33), and their lack of effector function, characterizing exhausted CD8 TL, as in human melanomas (34). An alternative, nonexclusive possibility is that adaptive immunity contributes to dampening excessive inflammatory responses (43).

Mela tumor development in mice equipped with an adaptive immune system may be related to the low expression of TA P1A and H-Ras^{G12V} by these tumors, contributing to low antigenicity and absence of inflammatory cytokine production, respectively. The reduced frequency of Mela tumor development in immunodeficient mice may be due to an unchecked overgrowth of Mela by Amela tumor. Mice bearing slowly progressing Mela tumors were not tolerized to TA expressed on Amela tumors because they were able to reject a transplanted tumor established from an induced melanoma. This differs from the SV40 T-antigen model where tolerization occurred at the premalignant stage concomitant with anti-SV40 T-antigen antibody production (14). The possibility that partial tolerance to low P1A-expressing Mela tumors may exist in Mela-bearing mice cannot be excluded, however. Amela and Mela tumors may also vary in their expression of other TAs.

Cancer-associated MPDs: Is there one culprit? In healthy individuals, IMCs (CD11b$^+$Gr1$^+$ in the mouse) generated in the BM differentiate into mature granulocytes, macrophages, and DC. In various pathologic situations, IMCs accumulate in lymphoid organs and can be recruited within tumors. It is thought that this occurs under the influence of factors that promote the expansion of IMC and inhibit their differentiation. Further, the activation of this IMC population within a given microenvironment seems to induce their acquisition of immunosuppressive activities, including those mediated by arginase-1, inducible nitric oxide synthase, reactive oxygen species, or peroxynitrite (7, 8).

G-CSF was detected both in tumor supernatants and systemically in mice with Amela tumors. It was previously found to be produced by aggressive human melanoma lines (44). This factor, which controls development of the granulocytic lineage, has been implicated in the recruitment of myeloid precursors from the BM (45) and in MPD when present at high serum levels (30). VEGFA, also detected in sera of Amela-bearing mice, has recently been implicated in cancer-associated MPD, including extramedullary hematopoiesis (46), extending its known effect on tumor vasculature. In addition to G-CSF and VEGFA, Amela tumors also produced CCL2, known to recruit CCR1- and CCR2-positive cells, including IMCs (47). None of these factors was produced by slow-progressing Mela tumors, consistent with the absence of tumor infiltration and of MPD in Mela-bearing mice.

Our results indicate that oncogenic progression in aggressive induced Amela melanomas is associated with production of factors that recruit precursors of myeloid cells from the BM and promote their growth. Within the tumor, immunosuppressive entities such as arginase-1 and cox2 are detected, as well as VEGFA, which may contribute to vascularization.

Relevance of the Amela-bearing mice as preclinical model. Pigmented melanomas can be very aggressive in patients, although in some studies aggressiveness was associated with downregulation of the expression of genes controlling melanocyte differentiation and pigmentation (48, 49). Whether Amela tumors represent a case of such de-differentiation requires further molecular analysis. Induced, Amela-bearing mice presenting a state of Th2/Th17-oriented chronic inflammation seem to recapitulate, in part, the Th2-dominant chronic inflammation observed in advanced melanoma patients (28), in which a cause-effect relationship was suggested between tumor-produced VEGF and systemic Th2 polarization.

The Amela tumor stage thus provides a model for testing modalities of adoptive immunotherapy or host conditioning (50), which may be efficient in the context of chronic inflammation. Further, the inducible character of the Amela tumor model will permit study of means to block progression toward a chronic inflammation after tumor induction. It may also be possible to determine whether particular tumor-produced cytokines/growth factors or signaling molecules (STAT3; ref. 23) are essential for tumor progression and/or tumor-associated immune dysfunction by deleting expression of candidate genes via the inducible Cre system of the TiRP mice.

Disclosure of Potential Conflicts of Interest

No potential conflicts of interest were disclosed.

Acknowledgments

We thank Lee Leserman and Nathalie Auphan-Anezin (Centre d'Immunologie de Marseille-Luminy) for numerous suggestions and the Centre d'Immunologie de Marseille-Luminy imaging and animal facilities personnel for assistance.

Grant Support

Institut National de la Sante et de la Recherche Medicale, Centre National de la Recherche Scientifique, INCA (MelanIm) and INCA-PROCAN program (A-M. Schmitt-Verhulst), European Communities (Integrated project "Cancerimmunotherapy" LSHC-CT-2006-518234; A-M. Schmitt-Verhulst and B. Van den Eynde), and "Association pour la Recherche sur le Cancer" (A-M. Schmitt-Verhulst). S.M. Soudja and M. Wehbe were doctoral fellows from Association pour la Recherche sur le Cancer.

The costs of publication of this article were defrayed in part by the payment of page charges. This article must therefore be hereby marked *advertisement* in accordance with 18 U.S.C. Section 1734 solely to indicate this fact.

Received 11/30/2009; revised 02/01/2010; accepted 02/22/2010; published OnlineFirst 04/20/2010.

Published OnlineFirst April 20, 2010; DOI: 10.1158/0008-5472.CAN-09-4354

References

1. Appay V, Jandus C, Voelter V, et al. New generation vaccine induces effective melanoma-specific CD8$^+$ T cells in the circulation but not in the tumor site. J Immunol 2006;177:1670–8.
2. Parmiani G, Castelli C, Santinami M, Rivoltini L. Melanoma immunology: past, present and future. Curr Opin Oncol 2007;19:121–7.
3. Boon T, Coulie PG, Van den Eynde BJ, van der Bruggen P. Human T cell responses against melanoma. Annu Rev Immunol 2006;24:175–208.
4. Mortarini R, Piris A, Maurichi A, et al. Lack of terminally differentiated tumor-specific CD8$^+$ T cells at tumor site in spite of antitumor immunity to self-antigens in human metastatic melanoma. Cancer Res 2003;63:2535–45.
5. Willimsky G, Blankenstein T. Sporadic immunogenic tumours avoid destruction by inducing T-cell tolerance. Nature 2005;437:141–6.
6. Khazaie K, von Boehmer H. The impact of CD4$^+$CD25$^+$ Treg on tumor specific CD8$^+$ T cell cytotoxicity and cancer. Semin Cancer Biol 2006;16:124–36.
7. Serafini P, Borrello I, Bronte V. Myeloid suppressor cells in cancer: recruitment, phenotype, properties, and mechanisms of immune suppression. Semin Cancer Biol 2006;16:53–65.
8. Gabrilovich DI, Nagaraj S. Myeloid-derived suppressor cells as regulators of the immune system. Nat Rev Immunol 2009;9:162–74.
9. Gabrilovich DI, Bronte V, Chen SH, et al. The terminology issue for myeloid-derived suppressor cells. Cancer Res 2007;67:425, author reply 6.
10. Mantovani A, Allavena P, Sica A, Balkwill F. Cancer-related inflammation. Nature 2008;454:436–44.
11. Olive KP, Jacobetz MA, Davidson CJ, et al. Inhibition of Hedgehog signaling enhances delivery of chemotherapy in a mouse model of pancreatic cancer. Science 2009;324:1457–61.
12. Demehri S, Turkoz A, Kopan R. Epidermal Notch1 loss promotes skin tumorigenesis by impacting the stromal microenvironment. Cancer Cell 2009;16:55–66.
13. Koebel CM, Vermi W, Swann JB, et al. Adaptive immunity maintains occult cancer in an equilibrium state. Nature 2007;450:903–7.
14. Willimsky G, Czeh M, Loddenkemper C, et al. Immunogenicity of premalignant lesions is the primary cause of general cytotoxic T lymphocyte unresponsiveness. J Exp Med 2008;205:1687–700.
15. de Visser KE, Korets LV, Coussens LM. *De novo* carcinogenesis promoted by chronic inflammation is B lymphocyte dependent. Cancer Cell 2005;7:411–23.
16. Uyttenhove C, Godfraind C, Lethe B, et al. The expression of mouse gene P1A in testis does not prevent safe induction of cytolytic T cells against a P1A-encoded tumor antigen. Int J Cancer 1997;70:349–56.
17. Kyewski B, Derbinski J. Self-representation in the thymus: an extended view. Nat Rev Immunol 2004;4:688–98.
18. Huijbers IJ, Krimpenfort P, Chomez P, et al. An inducible mouse model of melanoma expressing a defined tumor antigen. Cancer Res 2006;66:3278–86.
19. Shanker A, Auphan-Anezin N, Chomez P, Giraudo L, Van den Eynde B, Schmitt-Verhulst AM. Thymocyte-intrinsic genetic factors influence CD8 T cell lineage commitment and affect selection of a tumor-reactive TCR. J Immunol 2004;172:5069–77.
20. Shanker A, Verdeil G, Buferne M, et al. CD8 T cell help for innate antitumor immunity. J Immunol 2007;179:6651–62.
21. Chin L, Garraway LA, Fisher DE. Malignant melanoma: genetics and therapeutics in the genomic era. Genes Dev 2006;20:2149–82.
22. Chin L, Pomerantz J, Polsky D, et al. Cooperative effects of INK4a and ras in melanoma susceptibility *in vivo*. Genes Dev 1997;11:2822–34.
23. Yu H, Pardoll D, Jove R. STATs in cancer inflammation and immunity: a leading role for STAT3. Nat Rev Cancer 2009;9:798–809.
24. Kim HK, De La Luz Sierra M, Williams CK, Gulino AV, Tosato G. G-CSF down-regulation of CXCR4 expression identified as a mechanism for mobilization of myeloid cells. Blood 2006;108:812–20.
25. Nakayama T, Mutsuga N, Tosato G. Effect of fibroblast growth factor 2 on stromal cell-derived factor 1 production by bone marrow stromal cells and hematopoiesis. J Natl Cancer Inst 2007;99:223–35.
26. Awasthi A, Kuchroo VK. IL-17A directly inhibits TH1 cells and thereby suppresses development of intestinal inflammation. Nat Immunol 2009;10:568–70.
27. Hinrichs CS, Kaiser A, Paulos CM, et al. Type 17 CD8$^+$ T cells display enhanced antitumor immunity. Blood 2009;114:596–9.
28. Nevala WK, Vachon CM, Leontovich AA, Scott CG, Thompson MA, Markovic SN. Evidence of systemic Th2-driven chronic inflammation in patients with metastatic melanoma. Clin Cancer Res 2009;15:1931–9.
29. O'Connell RM, Rao DS, Chaudhuri AA, et al. Sustained expression of microRNA-155 in hematopoietic stem cells causes a myeloproliferative disorder. J Exp Med 2008;205:585–94.
30. Meixner A, Zenz R, Schonthaler HB, et al. Epidermal JunB represses G-CSF transcription and affects haematopoiesis and bone formation. Nat Cell Biol 2008;10:1003–11.
31. Galon J, Costes A, Sanchez-Cabo F, et al. Type, density, and location of immune cells within human colorectal tumors predict clinical outcome. Science 2006;313:1960–4.
32. Rodriguez PC, Hernandez CP, Quiceno D, et al. Arginase I in myeloid suppressor cells is induced by COX-2 in lung carcinoma. J Exp Med 2005;202:931–9.
33. Pentcheva-Hoang T, Corse E, Allison JP. Negative regulators of T-cell activation: potential targets for therapeutic intervention in cancer, autoimmune disease, and persistent infections. Immunol Rev 2009;229:67–87.
34. Ahmadzadeh M, Johnson LA, Heemskerk B, et al. Tumor antigen-specific CD8 T cells infiltrating the tumor express high levels of PD-1 and are functionally impaired. Blood 2009;114:1537–544.
35. Zippelius A, Batard P, Rubio-Godoy V, et al. Effector function of human tumor-specific CD8 T cells in melanoma lesions: a state of local functional tolerance. Cancer Res 2004;64:2865–73.
36. de Visser KE, Eichten A, Coussens LM. Paradoxical roles of the immune system during cancer development. Nat Rev Cancer 2006;6:24–37.
37. Prehn RT. Stimulatory effects of immune reactions upon the growths of untransplanted tumors. Cancer Res 1994;54:908–14.
38. Soucek L, Lawlor ER, Soto D, Shchors K, Swigart LB, Evan GI. Mast cells are required for angiogenesis and macroscopic expansion of Myc-induced pancreatic islet tumors. Nat Med 2007;13:1211–8.
39. Lin EY, Li JF, Gnatovskiy L, et al. Macrophages regulate the angiogenic switch in a mouse model of breast cancer. Cancer Res 2006;66:11238–46.
40. DeNardo DG, Barreto JB, Andreu P, et al. CD4(+) T cells regulate pulmonary metastasis of mammary carcinomas by enhancing protumor properties of macrophages. Cancer Cell 2009;16:91–102.
41. Ambrosino E, Spadaro M, Iezzi M, et al. Immunosurveillance of Erbb2 carcinogenesis in transgenic mice is concealed by a dominant regulatory T-cell self-tolerance. Cancer Res 2006;66:7734–40.
42. Spiotto MT, Rowley DA, Schreiber H. Bystander elimination of antigen loss variants in established tumors. Nat Med 2004;10:294–8.
43. Guarda G, Dostert C, Staehli F, et al. T cells dampen innate immune responses through inhibition of NLRP1 and NLRP3 inflammasomes. Nature 2009;460:269–73.
44. Safarians S, Rivera SP, Sternlicht MD, Naeim F, Barsky SH. Ectopic G-CSF expression in human melanoma lines marks a trans-dominant pathway of tumor progression. Am J Pathol 1997;150:949–62.
45. Shojaei F, Wu X, Qu X, et al. G-CSF-initiated myeloid cell mobilization and angiogenesis mediate tumor refractoriness to anti-VEGF therapy in mouse models. Proc Natl Acad Sci U S A 2009;106:6742–7.
46. Xue Y, Religa P, Cao R, et al. Anti-VEGF agents confer survival advantages to tumor-bearing mice by improving cancer-associated systemic syndrome. Proc Natl Acad Sci U S A 2008;105:18513–8.
47. Sawanobori Y, Ueha S, Kurachi M, et al. Chemokine-mediated rapid turnover of myeloid-derived suppressor cells in tumor-bearing mice. Blood 2008;111:5457–66.
48. Ryu B, Kim DS, Deluca AM, Alani RM. Comprehensive expression profiling of tumor cell lines identifies molecular signatures of melanoma progression. PLoS One 2007;2:e594.
49. Salti GI, Manougian T, Farolan M, Shilkaitis A, Majumdar D, Das Gupta TK. Micropthalmia transcription factor: a new prognostic marker in intermediate-thickness cutaneous malignant melanoma. Cancer Res 2000;60:5012–6.
50. Powell DJ Jr., Dudley ME, Hogan KA, Wunderlich JR, Rosenberg SA. Adoptive transfer of vaccine-induced peripheral blood mononuclear cells to patients with metastatic melanoma following lymphodepletion. J Immunol 2006;177:6527–39.

AACR American Association for Cancer Research

Cancer Research

The Journal of Cancer Research (1916–1930) | The American Journal of Cancer (1931–1940)

Tumor-Initiated Inflammation Overrides Protective Adaptive Immunity in an Induced Melanoma Model in Mice

Saïdi M. Soudja, Maria Wehbe, Amandine Mas, et al.

Cancer Res Published OnlineFirst April 20, 2010.